Anni Rahko

PET IMAGING OF NEUROENDOCRINE NEOPLASMS

Advanced Studies Thesis
Spring Semester 2024

Anni Rahko

PET IMAGING OF NEUROENDOCRINE NEOPLASMS

Department of Clinical Physiology and Nuclear Medicine

Supervisor Head of Department Marko Seppänen

The originality of this thesis has been checked in accordance with the University of Turku quality assurance system using the Turnitin OriginalityCheck service.

UNIVERSITY OF TURKU
Faculty of Medicine

RAHKO, ANNI: PET Imaging of Neuroendocrine Neoplasms

Advanced Studies Thesis, 40 p.
Nuclear Medicine
January 2024

Positron emission tomography (PET) has a vital role in the diagnostics and therapeutics of neuroendocrine neoplasms (NEN). NEN form a diverse group of neoplasms that arise from the cells of neuroendocrine origin. The incidence of NEN is rising mainly due to improved diagnostics. PET is a nuclear imaging modality widely used in the imaging of NEN. PET imaging utilizes radiolabeled tracers that concentrate in the tumor cells more than normal organs. Today, these radiotracers are under intense investigations. The heterogenous nature of NEN creates the need for a variety of different radiopharmaceuticals. Some radiotracers pose also economic and logistic challenges, so novel solutions are needed. In Turku PET Center, valuable investigations are being conducted regarding the PET imaging of NEN.

This thesis is a literature review where the aim is to study the most used PET radiotracers and their indications in the management of NEN. Firstly, a closer look is taken into the characteristics of NEN as well as the technical principles of PET for a more thorough understanding. The full names of PET radiotracers are complex, so abbreviations are used first containing the positron emitter followed by an acronym of the molecule. In this literature review, the discussed radiotracers are ^{68}Ga-labeled somatostatin analogues (SSA), ^{18}F-FDG, ^{18}F-DOPA, and exendin-4. A promising newcomer in the field,^{18}F-SiTATE, will be discussed more profoundly. ^{18}F-SiTATE is being studied in Turku PET Center, and it could possibly replace the widely used ^{68}Ga-DOTANOC. Radiopharmaceuticals are also used in the peptide receptor radionuclide therapy (PRRT) of NEN.

According to literature, the location of the primary tumor is relevant in the determination of the most appropriate radiotracer. Radiotracers have different affinity profiles to receptors on cell membranes. The uptake of a radiotracer in tumor cells represents the receptor profile of the disease. NEN are most often met in the gastrointestinal tract. For well-differentiated gastrointestinal NEN, ^{68}Ga-labeled SSA is the most suitable option whereas ^{18}F-FDG detects poorly differentiated neuroendocrine carcinomas (NEC). PET is also needed for the evaluation of appropriate therapies for NEN patients. Regarding PRRT, ^{177}Lu-DOTATATE is the preferred radiotracer, but ^{90}Y-DOTATATE is also used. New radiopharmaceuticals for the diagnostics and therapeutics of NEN are under eager investigations. More research is needed on the eligibility of ^{18}F-SiTATE, but the preliminary data is promising.

Keywords: neuroendocrine neoplasms, PET-CT, somatostatin receptor imaging

TABLE OF CONTENTS

1 ABBREVIATIONS

CEA	Carcinoembryonic antigen
CS	Carcinoid syndrome
CT	Computed tomography
^{18}F-FDG	^{18}F-fluoro-6-deoxy-glucose
^{18}F-SiTATE	^{18}F-SiFAlin-Asp$_3$-PEG$_1$-TATE
^{18}F-DOPA	6-l-^{18}F-fluoro-dihydroxyphenylalanine
^{68}Ga-DOTANOC	[^{68}Ga-DOTA^0-^{1}NaI^3]octreotide
^{68}Ga-DOTATATE	[^{68}Ga-DOTA^0 -Tyr^3]octreotate
^{68}Ga-DOTATOC	[^{68}Ga-DOTA^0 -Tyr^3] octreotide
GEP-NEN	Gastroenteropancretic neuroendocrine neoplasm
GLP-1R	Glucagon-like peptide-1 receptor
HH	Hyperinsulinemic hypoglycemia
LCNEC	Large cell neuroendocrine carcinoma
LOR	Line of response
MEN1/2	Multiple endocrine neoplasia type 1/2
MRI	Magnetic resonance imaging
MTC	Medullary thyroid carcinoma
NEC	Neuroendocrine carcinoma
NEN	Neuroendocrine neoplasm
PET	Positron emission tomography
PNET	Pancreatic neuroendocrine tumor
PPGL	Phaeochromocytomas and paragangliomas
PRRT	Peptide receptor radionuclide therapy
SCLC	Small cell lung carcinoma
SPECT	Single-photon emission computed tomography
SRI	Somatostatin receptor imaging
SSA	Somatostatin analogue
SSTR	Somatostatin receptor
SUV	Standardized uptake value
VIP	Vasoactive intestinal peptide
VOI	Volume of interest

2 INTRODUCTION

Neuroendocrine neoplasms (NEN) form a diverse group of neoplasms that arise from cells of neuroendocrine origin. The most common locations of NEN are the gastrointestinal tract and the lungs, but they can arise from all around the body. Roughly, NEN are classified into well and poorly differentiated tumors using Ki67 index. Some NEN can produce hormones leading to varying clinical pictures. They are also linked to hereditary predisposing mutations. As NEN are a complex group of tumors, this literature review will summarize their most important characteristics. During the past decades, the incidence of NEN has risen most likely due to advancements in their diagnostics. Nuclear medicine plays a relevant role in the diagnostic work-up as well as the clinical management of NEN.

Positron emission tomography (PET) is a nuclear imaging technique widely used in the imaging of NEN. PET imaging has been shown to surpass single photon emission computed tomography (SPECT), which was formerly a widely established imaging method. Today, SPECT is recommended only when PET is not available, thus SPECT will be only briefly discussed. PET scanning is combined often with computer tomography (CT) scan or less frequently with magnetic resonance imaging (MRI). PET-CT/MRI offers more accurate information of the anatomical location of the tumor than a PET image alone. PET imaging utilizes radiotracers that concentrate in tumor cells more than in normal organs. The focus in this review will be in these radiotracers used in the PET imaging of NEN. The technical principles of PET will also be discussed.

The aim of this literature review is to investigate PET radiotracers and their indications in the diagnostics and therapeutics of NEN. The spectrum of PET radiotracers is wide. This review examines ^{68}Ga-labeled somatostatin analogues (SSA), ^{18}F-FDG, ^{18}F-DOPA, and exendin-4, as well as the newcomer ^{18}F-SiTATE which will be more thoroughly discussed. ^{18}F-SiTATE is currently being studied in Turku PET Center. The full names of PET radiotracers are complex, so abbreviations are used first containing the positron emitter followed by an acronym of the molecule. Radiotracers have different affinity profiles to receptors on cell membranes. Hence, the uptake of a radiotracer in tumor cells represents the receptor profile of the disease.

LITERATURE REVIEW

2.1 WHAT ARE NEUROENDOCRINE NEOPLASMS?

2.1.1 CLASSIFICATION

Neuroendocrine neoplasms (NEN) are a heterogenous group of relatively rare neoplasms that emerge from cells of neuroendocrine origin. These neoplasms arise from nerve structures, endocrine organs, such as the pituitary, and the adrenal glands, or the diffuse neuroendocrine system that consist of neuroendocrine cells scattered throughout the body. Therefore, almost every organ of the body can host neuroendocrine neoplasms. The most common locations of NEN are the gastrointestinal tract, especially the appendix, ileum, and rectum, as well as the lungs and the pancreas. NEN can spread to the surrounding tissues and metastasize to the lymph nodes, the liver, and the bones. (Arola, Haglund and Välimäki, 2010; Inzani and Rindi, 2021; Rindi *et al.*, 2022)

The classification of NEN was very recently (2022) updated by the World Health Organization. Today, the classification is based on differentiation and proliferative grading. NEN express biomarkers of neuroendocrine differentiation. The two most important biomarkers are chromogranin A and synaptophysin. Also, NEN express hormones resembling structural and functional characteristics, as well as transcription factors identifying the origin of metastatic lesions. These biomarkers are used in detection, diagnostics, and classification of NEN in immunohistochemical staining. Histological diagnosis is mandatory. (Inzani and Rindi, 2021; Rindi *et al.*, 2022)

The current grading system classifies NEN to neuroendocrine tumors (NET) and neuroendocrine carcinomas (NEC). NET are further classified into three grades, where grade 1 (G1) is the least aggressive and grade 3 (G3) the most aggressive form. Generally, NET are well-differentiated tumors meaning that the tumor cells resemble their non-neoplastic counterparts. On the other hand, NEC are poorly differentiated, so they display with deranged genetic and molecular profiles, severe cellular atypia as well as disordered growth. NEC are further classified into small and large cell types. The classification of NEN into NET and NEC mirrors their genetic differences: NET have a low mutational burden

whereas NEC display high degree of gene alterations. A challenge we face today is the distinction of grade 3 NET from NEC. (Rindi *et al.*, 2022)

The grading system of NEN is based on Ki67 proliferation index and mitotic rate. The Ki67 is a nuclear protein generally expressed only in proliferating cells. The current system enables identification of a well-differentiated NET with G3 proliferative values from NEC. Criteria for grade 1 gastrointestinal or lung NET are Ki67 index below 3% and/or less than 2 mitoses per 2 mm^2. Grade 2 tumors have Ki67% 3-20% and/or 2-20 mitoses per 2 mm^2. If Ki67 index is over 20% and/or over 20 mitoses are seen per 2 mm^2, the tumor is grade 3. This division is illustrated in Table 1. Tumor necrosis is used as a grading parameter in many NEN types excluding gastrointestinal and pancreaticobiliary NEN. (Rindi *et al.*, 2022) Also, Ki67 index is used in choosing the optimal PET radiotracer, but more on this later.

Table 1. A simplified classification of NEN based on the proliferation index (Ki67%) and the number of mitoses seen in histology. NET = neuroendocrine tumor, NEC = neuroendocrine carcinoma. (Rindi *et al.*, 2022)

Type	Grade	Ki67%	Mitoses / 2mm^2
NET	G1	< 3	< 2
	G2	3-20	2-20
	G3	> 20	> 20
NEC		> 20	> 20

Besides the above-mentioned division, classification of NEN acknowledges few more classes of NEN. Mixed neuroendocrine-non-neuroendocrine tumors (MiNEN) are epithelial tumors consisting of a neuroendocrine and a non-neuroendocrine component and can arise anywhere in the body, but they should be further specified with a site-specific terminology that indicates the different combinations of tumor components. Amphicrine tumors have neuroendocrine and non-neuroendocrine differentiation in the same cells, and they are capable of both exocrine and neuroendocrine secretion of hormones. Composite paraganglioma/neuroma and neuroendocrine tumor (CoGNET) is an unusual tumor consisting of paraganglioma or ganglioneuroma with a duodenal NET. (Rindi *et al.*, 2022)

2.1.2 EPIDEMIOLOGY

Neuroendocrine neoplasms are a rare group of tumors, but their incidence is rising. The incidence of NEN is around 8/100 000 in one year and has been rising during the past decades most likely due to improved diagnostics, higher awareness, and improved classification. In Finland, around 230 new NEN cases are reported yearly. NEN are met most in the gastroenteropacreatic (GEP) tract (approximately 72% of all NEN). The second most common location is the bronchopulmonary system (approximately 25% of NEN). The rest can originate from a variety of sites around the body. The prognosis is rather good, which leads to a rise in the incidence as well. The clinical course of the disease can be heterogenous. NEN can be asymptomatic for years leading to diagnosis at a late stage (especially GEP-NEN) when the disease is already locally advanced or metastasized. At the moment of diagnosis, 50% of NEN are localized and 40% have already metastasized. (Kauhanen *et al*., 2020; Janson *et al.*, 2021).

2.1.3 CLINICAL PICTURE

The clinical picture of a NEN is often asymptomatic or presents with non-specific symptoms. NEN are classified as functional or non-functional based on whether they secrete hormones or not. Non-functional NEN often express hormones at immunohistochemistry but are unable to release them. Non-functional NEN can present themselves in several ways. They can cause upper abdominal complaints or tumor mass symptoms. Esophageal NEN presents with dysphagia and hoarseness. Tumors of the pancreatic head can lead to extrahepatic jaundice. NEN in the jejunum or ileum can present with pseudo-obstruction or intestinal hemorrhage. Appendiceal NEN is nearly always found due to the surgery performed to treat appendicitis. Additionally, NEN of the colon are often an incidental finding in colonoscopy. (Arola, Haglund and Välimäki, 2010; Inzani and Rindi, 2021; Rindi *et al.*, 2022) (Janson *et al.*, 2021)

Functional NEN are less rare than non-functional, and release hormones excessively which leads to different syndromes related to the specific hormone overexcretion. Some of the most common types of hormone secreting tumors, their leading symptoms, and the

related syndromes are presented in Table 2. Functional NEN are usually well-differentiated. As mentioned earlier, the most common locations of NEN are the appendix, small intestine, rectum, lungs, and pancreas. In the duodenum, gastrinoma and somatostatinoma are the most common tumor types, but sometimes serotonin or calcitonin producing tumors are seen. Most NEN of the pancreas are non-functional, but of the functional pancreatic NEN insulin and gastrin-producing tumors are the most common. NEN of the lungs can lead to carcinoid syndrome or Cushing syndrome though it is extremely rare. Also, NEN can secrete other hormones and substances such as growth-hormone-releasing hormone (GHRH), antidiuretic hormone (ADH), histamine, pancreatic polypeptide, and PTH-like peptide (PLP) among others. (Arola, Haglund and Välimäki, 2010; Inzani and Rindi, 2021; Janson *et al.*, 2021; Dam *et al.*, 2023)

Table 2. The different hormones secreted by functional NENs, their leading symptoms, and the related syndromes. VIP = vasoactive peptide; ACTH = adrenocorticotropic hormone; CRH = corticotropin-releasing hormone; GHRH = growth hormone releasing hormone. (Arola, Haglund and Välimäki, 2010; Hofland *et al.*, 2019; Janson *et al.*, 2021; Dam *et al.*, 2023)

Hormone	Tumor / Related syndrome	Main symptoms
Gastrin	Gastrinoma / Zollinger-Ellison syndrome	Peptic ulcer disease
Insulin	Insulinoma / hyperinsulinemic hypoglycemia	Hypoglycemia
Glucagon	Glucagonoma	Necrotic skin rush
VIP	Vipoma / Verner-Morrison syndrome	Watery diarrhea, hypokalemia, acidosis
Somatostatin	Somatostatinoma	Gall stones, steatorrhea, impaired glucose tolerance, hypochlorhydria
Serotonin and tachykinins	Carcinoid syndrome	Flushing, diarrhea, bronchospasm, heart disease, carcinoid crisis
ACTH or CRH	Cushing syndrome	Weight gain, “moon face”, hypertension, thin skin, muscle weakness
GHRH	Acromegaly	Enlargement of the body extremities

Carcinoid syndrome (CS) is a disease caused by functioning neuroendocrine tumors. Typical symptoms are vasoactive flushing, diarrhea, bronchospasms, and heart disease. It is caused by secretion of serotonin and tachykinins. The inactive form of serotonin, 5-hydroxyindolacetid acid (5-HIAA) is used the diagnosis of CS. The syndrome is commonly met in patients with midgut NET, but it can present with NET in other organs as well. Carcinoid crisis is an acute precipitation of carcinoid syndrome. The clinical picture of carcinoid crisis includes hypotension/hypertension, arrhythmia, bronchospasm, and

symptoms of the central nervous system. This phenomenon is caused by the sudden release of hormones following damage to tumor cells, for example due to different treatments. Neuroendocrine carcinomas (NEC) tend to present with more aggressive clinical picture than NET. Everything considered, the clinical picture of a NEN varies and can be unspecific and misleading. (Arola, Haglund and Välimäki, 2010; Hofland *et al.*, 2019; Basu *et al.*, 2020)

2.1.4 GENETICS

Although most NEN are sporadic, hereditary predisposing mutations are common in patients with neuroendocrine tumors. NEN are associated with syndromes due to these inherited mutations. Most of the syndromes involve multiple organs. The most common germline susceptibility is a loss-of-function mutation in a tumor suppressor gene. Genetic testing should be performed with patients with a family background of NEN, multiple endocrine neoplasia (MEN-syndrome), or features suspicious of a hereditary disease. (Aittomäki and Peltomäki, 2016; Giovanella *et al.*, 2020). Patients with hereditary syndromes can be diagnostically particularly challenging. (Rindi *et al.*, 2022)

Multiple endocrine neoplasia (MEN) types 1 and 2 are the most recognized forms of endocrine tumor susceptibility. MEN1 syndrome is due to a mutation in MEN1-gene. Endocrine tumors in the pituitary, pancreas and GI-tract are common, but almost all patients develop hyperparathyroidism and following hypercalcemia. MEN2 syndrome predisposes to medullary thyroid carcinoma (MTC) as well as to phaeochromocytoma and hyperparathyroidism. MEN2 is due to activated RET oncogene. Also, MEN2 syndrome can be further divided into A and B forms. Von Hippel-Lindau syndrome is caused by a mutation in the VHL gene and predisposes to phaeochromocytomas. (Aittomäki and Peltomäki, 2016; Taïeb *et al.*, 2019; Giovanella *et al.*, 2020)

2.2 IMAGING OF NEUROENDOCRINE TUMORS

2.2.1 PRINCIPLES OF PET

2.2.1.1 PHYSICAL AND TECHNICAL PRINCIPLES OF PET

Positron emission tomography (PET) is a quantitative imaging technique that allows non-invasive assessment of functional and biological processes. PET is especially used in cancer diagnostics and treatments. The mechanism is to measure the distribution of a radiotracer in vivo. In the performance of PET imaging, the radiotracer is injected to the patient and then accumulates in tissue. These tracers are positron emitting tracers which are also called beta emitters. The radioactive atom of the radiotracer emits protons which are formed in the process of nuclear decay. During nuclear decay protons are converted into a neutrino, a neutron, and a positron. (Komar, 2012) (Hogg and Testanera, 2010)

After travelling a distance up to few millimeters, prositrons combine with an electron. As positron and electron are each other's antiparticles, they react in a process called annihilation where the particles are turned into energy. In consequence, two gamma photons are emitted to nearly opposite directions. These photons are detected simultaneously forming the basis of PET image formation. The photons are detected by a ring of detectors surrounding the object or subject. The ring of detectors separates true events from random by registering the time and energy windows of the photons. (Komar, 2012) (Hogg and Testanera, 2010)

The horizontal axis between the simultaneously detected photons at opposite sides of the detector ring is called the line of response (LOR). The simultaneously detected photons define a coincidence event. The LOR is used in the production of a sinogram which is a visual representation from the raw data. Before imagine reconstruction, the raw data needs attenuation correction as attenuation can reduce the amount of true coincidence events. Altogether, the detectors are composed of scintillator crystals and photomultiplier tubes which convert gamma radiation into visible light. Afterwards, the light signals are transformed into a digital form which is then further processed. (Silvoniemi, 2018)

2.2.1.2 QUANTIFICATION OF PET DATA

The quantification of PET data needs mathematical modelling. The standardized uptake value (SUV) is the most widely used parameter for the analysis of most PET radiotracers. However, SUV is not directly comparable between institutions or patients. The reasons for this are discussed shortly. Standard image analysis is based on determining tracer uptake in the volume of interest (VOI). SUV is the ratio between the radiotracer's concentration in the certain VOI and the injected activity divided by a normalization value. The normalization value is most often the body mass but can be replaced with the lean body weight (only for ^{18}F-FDG) or the body surface area. Regarding the calculation of the SUV, see Equation 1. (Silvoniemi, 2018)

$$SUV = \frac{activity\ concertration\ (\frac{kBq}{ml})}{injected\ activity\ (MBq)/\ body\ mass\ (kg)}$$

Equation 1. The standardized uptake value (SUV). The normalization value is presented here as the body mass, but it can be replaced with body surface area or lean body weight. (Silvoniemi, 2018)

In its simplicity, the SUV is widely used in clinical cancer imaging. Activity concentration is calculated by scanning the patient for a certain time interval after a predefined time after the radiotracer injection. In addition to mean SUV (SUV_{mean}) of the whole VOI, maximum SUV (SUV_{max}) is also commonly determined from the voxel of the highest uptake. The limitations of SUV are the many confounding factors such as alternations in body metabolism, timing of the data acquisition and image reconstruction. The data presented as SUV units is not directly comparable between patients or institutions due to these confounding factors. Efforts have been made to decrease the variability of PET image quantification, but any specific SUV reference values have not been defined for the differential diagnosis of lesions. (Silvoniemi, 2018)

Other more accurate quantification methods of PET data have been developed. The most used methods are multiple-time graphical analysis (MTGA) and compartmental modelling. These methods provide quantitative measures of true physiological processes. However, the more accurate the method, the more effort is required in terms of image acquisition and post-acquisition processing. The use of the above-mentioned methods requires modified imaging protocols as well as blood sampling making the data acquisition more

expensive, time-consuming, and more uncomfortable for the patient. Hence, these methods are rarely used in diagnostic work. (Komar, 2012)

2.2.1.3 PET-CT HYBRID IMAGING

The PET data can be used in combination with data from computed tomography (CT). PET-CT hybrid imaging has become established modality in clinical practice. PET-CT is a multimodality or integrated physical combination of PET and CT. Coupled through hardware fusion, PET-CT enables a single scan where the patient is positioned only once, and improved registration accuracy. PET-CT from the skull base to midthigh is standard covering most of the relevant parts of the body in oncology. Different types of CT scan can be included in PET-CT. Diagnostics CT scans can be performed with or with-out contrast enhancement. The image quality in contrast-enhanced CT is better in comparison with contrast-free images. (Hogg and Testanera, 2010; Pietrzak, 2021)

Combining PET with CT has many advantages. The functional images of PET have relatively poor spatial resolution. PET-CT combines the functional information of PET and the superior spatial resolution of CT. Together PET and CT allow for better anatomical localization and characterization of lesions as well as better evaluation of pathological processes. PET scan can also be combined with magnetic resonance imaging (MRI). (Komar, 2012; Pietrzak, 2021)

2.2.1.4 IMAGE INTERPRETATION AND PITFALLS

The interpretation of PET images requires extensive knowledge of the normal distribution of radiotracers and physiological variation. Physiological uptake of PET radiotracers is most intensely seen in the bladder, kidneys, spleen, and liver. Firstly, the imaging procedure should be high-quality to ensure optimal image for interpretation. The imaging procedure consists of patient preparation, administration of the radiotracer, and acquisition of the image. Suboptimal technologist practice might lead to difficulties in interpretation and, furthermore, to misdiagnosis. (Bozkurt *et al.*, 2017; Pietrzak, 2021)

Secondly, the one should be mindful of false positive and false negative results. The causes of false results vary according to the used radiotracer. ^{68}Ga-DOTA-conjugated tracers are currently the golden standard in the PET-CT imaging of NEN. Uptake of these tracers is not specific for malignant tumors but also encountered at sites of infection and inflammation which results in false positive findings. Additionally, the dedifferentiation or the lesions' small size might lead to false negative findings. When ^{68}Ga-DOTA-conjugated tracers are used, somatostatin analogue therapy or endogenous production of somatostatin may also interfere with tumor detection. (Bozkurt *et al.*, 2017)

Thirdly, the clinical context of the image is important. This consists of the clinical question leading to the performance of the imaging, patient's clinical history and recent results of biochemical tests. The radiotracers show variable sensitivity in different tumor types. In conclusion, focal tracer uptake in PET image that cannot be explained by physiologic biodistribution is to be considered pathologic, and similar finding in CT supports this conclusion. (Bozkurt *et al.*, 2017; Pietrzak, 2021)

There is a heap of technical pitfalls related to PET-CT imaging in general as well as pitfalls specific to a certain radiotracer. Movement artefacts can be detrimental to the quality of a PET-CT image. PET-CT allows for better anatomical localization of lesion than PET image alone. If attenuation correction is based on CT, there is a risk of overestimating the activity of the radiotracer. Misregistration between CT and PET images can lead to the superimposition of radiotracer activity on the wrong anatomical structure. (Bozkurt *et al.*, 2017; Pietrzak, 2021)

2.2.1.5 RADIOATION EXPOSURE

Nuclear imaging leads to radiation exposure to the patient. The development of PET and CT scanner has led to more rapid imaging and better image resolution with lower radiation exposure. Though, the main limitation of new generation scanners is the relatively high cost. The radiation exposure and protection from the radiation should always be considered before imaging. In PET imaging, the ionizing radiation is caused by the radionuclide injected into the patient and, also by the CT scan which is usually done in combination with PET. (Pietrzak, 2021). Effective dose (ED) represents the health risk to the

whole body caused by one imaging study. The ED is 3.2 mSv for 150 MBq injected activity for the established ^{68}Ga-DOTATATE and 7.0 mSv for 370 MBq injected activity for ^{18}F-FDG. (Bozkurt *et al.*, 2017). For comparison, the average annual environmental radiation dose in Finland is 5.9 mSv. (Environmental radiation. STUK. www.stuk.fi).

2.2.2 RADIOTRACERS IN THE IMAGING OF NEN

2.2.2.1 PRODUCTION OF RADIOTRACERS

To produce the radiotracers, radioactive isotopes are needed. As for the isotopes, they are produced with a particle accelerator called a cyclotron or a radionuclide generator. The most used isotopes in the imaging of NENs are fluorine-18 and gallium-68. For example, fluorine-18 is produced by bombarding oxygen-18-enriched water with protons. Elution of gallium-68 requires a ^{68}Ge/^{68}Ga generator. The isotopes suitable for PET imaging must have certain qualities, such as emitting positrons when they decay, having an appropriate half-life and having the ability to be synthetized into a pharmaceutical. There are some economic and logistic difficulties related to the production of radiotracers which is why new radiotracers with more favorable characteristics are still needed. (Pietrzak, 2021)

2.2.2.2 SSTR-TARGETING RADIOTRACERS

Radiotracers targeting somatostatin receptors (SSTR) have brought new vision to the imaging of neuroendocrine tumors. SSTR are G-protein-coupled receptors expressed in majority of NEN. Somatostatin receptors bind somatostatin which is a cyclic neuropeptide found for example in the central and peripheral nervous systems and endocrine cells. Somatostatin receptor (SSTR) expression differs greatly between different types of NEN. SSTR have multiple subtypes (SSTR1-SSTR5) SSTR2 being the most overexpressed among NEN. Endogenous somatostatin has the half-life of few minutes, hence synthetic somatostatin analogs (SSA) have been developed for clinical use. (Inzani and Rindi, 2021; Rindi *et al.*, 2022) (Hope *et al.*, 2023)

Currently, the SSTR targeting radiotracers in use are ^{68}Ga-DOTA-conjugated peptides (68Ga-1,4,7,10-tetraazacyclododecane-1,4,7,10-tetraacetic acid aka. DOTA) ^{68}Ga-DOTATOC, and ^{68}Ga-DOTATATE and ^{68}Ga-DOTANOC as well as copper-64-labeled ^{64}Cu-DOTATATE. The synthesis of gallium-68 requires 68Ge/68Ga generator. Ga-labelled somatostatin analogs bind to SSTR2. Also, different radiotracers have varying affinity profiles to SSTR3 and 5 as well. SSTR-PET is a key method in the diagnostics, localizing, stating, restaging, and therapy of all well-differentiated NEN. Though, the affinity and binding to receptors differs between SSTR-PET radiotracers they can be considered equivalent in terms of the ability to detect somatostatin receptor positive diseases. Currently, PET-CT with ^{68}Ga-DOTA-labeled tracers is the golden standard for the imaging of NEN. (Giovanella *et al.*, 2020; Kauhanen *et al*., 2020; Inzani and Rindi, 2021; Rindi *et al.*, 2022).

2.2.2.3 ^{18}F-DOPA AND ^{18}F-FDG

Other metabolic and molecular targets can be used in the imaging on NEN than somatostatin analogues. The target of ^{18}F-DOPA is the transport and decarboxylation of DOPA which is an amino acid. ^{18}F-DOPA is picked up by L-type amino acid transporter (LAT) and decarboxylated by aromatic amino acid decarboxylase (AADC). Synthesis of ^{18}F-DOPA is problematic as it is characterized by low labelling efficiency. The use of ^{18}F-DOPA (^{18}F-fluoro-dihydroxyphenylalanine) has declined, but it is still used in the imaging of NEN with low or variable expression of SSTR or high expression of LAT and AADC, such as in the imaging of medullary thyroid carcinoma (MTC) and pheochromocytoma. (Giovanella *et al.*, 2020; Kauhanen *et al*., 2020)

^{18}F-FDG (fluorine-18-fluorodeoxyglucose) is a modified glucose molecule labeled with radioactive fluorine-18. Preparation of ^{18}F-FDG can be done in-house or in a “ready-to-use” manner. As ^{18}F-FDG is taken up by cells the same way as glucose molecules, it depicts the glucose consumption of the area of interest and therefore its metabolic activity. ^{18}F-FDG accumulates in cells that express GLUT-transporters and hexokinase. ^{18}F-FDG is used with tumors with poor differentiation and/or Ki67 index exceeding 20%. Studies have shown that ^{18}F-FDG positivity predicts poorer prognosis and more aggressive disease. (Giovanella *et al.*, 2020; Kauhanen *et al*., 2020)

2.2.2.4 EXENDIN-4

A newcomer in the field is ^{68}Ga-exendin-4. Exendin-4 is an agonist to glucagon-like peptide-1 receptor (GLP-1R) that are expressed in the pancreas. GLP-1R based imaging has presented with high sensitivity for the detection of pancreatic insulinomas compared to other imaging modalities. Turku PET Center took part in the European BetaCure multicenter trial investigating the role of GLP-1R based imaging in localizing the focus of the disease in hyperinsulinemic hypoglycemia. The study showed that GLP-1R-PET is a viable tool in the clinical diagnostics of hyperinsulinemic hypoglycemia. (Kauhanen *et al*., 2020; Shah *et al.*, 2021)

2.2.2.5 DUAL TRACER PET-CT

Dual tracer PET-CT is performed with both ^{68}Ga-DOTATE and ^{18}F-FDG allowing exploration of dynamic tumor biology which is important before treatment decision making. As NEN are heterogenous tumors, the proliferation index of metastases can be different compared to the primary tumor, and the value can chance during the progression of the disease. The relative uptake of ^{68}GaDOTATE and ^{18}F-FDG in lesions forms a parameter that can be used besides the traditional Ki67 index in personalizing treatment strategies. Dual tracer PET-CT is useful in investigating the biology of tumors with Ki67 index between 10-20% as well 20-30%. Considering the latter interval, distinguishing between NET G3 from NEC is of great importance from management viewpoints. Also, discordance between dual tracer PET-CT and Ki67 can bring valuable information of the disease. (Basu *et al.*, 2020; Kauhanen *et al*., 2020)

2.2.2.6 ^{18}F-SiTATE

Presently, in Turku PET Center, a new radiotracer ^{18}F-SiTATE is being investigated to possibly replace the golden standard ^{68}Ga-DOTANOC in the imaging of SSTR-positive NEN. ^{18}F-SiTATE (previously known as ^{18}F-SIFA*lin*-TATE) is a positron emitter fluorine-18-labelled SSA targeting SSTR. The appeal of ^{18}F-SiTATE is the favorable characteristics of fluorine-18 compared with gallium-68. First-line studies conducted have presented with promising results showing no side effects in mice models or humans. Clinical

in-human data is still limited but recent studies indicate high tumor uptake values as well as high image quality. More on ^{18}F-SiTATE at the end of this literature review. (Ilhan *et al.*, 2019, 2020)

2.2.3 PET IMAGING OF NEUROENDOCRINE NEOPLASMS

PET imaging has a central role in the imaging of neuroendocrine tumors. The advantages of PET scanning are its high sensitivity and high spatial resolution. As discussed earlier, PET is a quantitative imaging technique that enables the non-invasive assessment of functional and biological processes by measuring the distribution of a radiotracer. The radiotracer is injected into the patient and then accumulates in tissue. Currently, many different radiotracers are in consistent use in the PET imaging of neuroendocrine tumors. These radiotracers utilize the varying characteristics of different types of neuroendocrine tumors in their diagnostics and therapeutics.

PET scan is almost always done in combination with computer tomography (CT) or sometimes with magnetic resonance imaging (MRI). CT is used to generate high-quality anatomical images. Hence, the advantaged of PET-CT are the exact anatomical localization and evaluation of pathological processes. As NEN frequently metastasize to the liver, PET-MRI can sometimes be used in the imaging of liver-dominant NENs with hepatobiliary MRI. Additionally, MRI is a non-ionizing imaging modality which is why it is favored when imagining children to greatly reduce the radiation dose. Also, endoscopic ultrasound can be used in the detection of the primary tumor and investigating the distribution of the disease. (Arola, Haglund and Välimäki, 2010; Hogg and Testanera, 2010; Janson *et al.*, 2021; Hope *et al.*, 2023)

Formerly, single photon emission computed tomography (SPECT) was widely established imaging method of NEN. The radiotracer used in SPECT imaging of NEN is indium-111-labelled somatostatin analog. This modality is known as OctreoScan. Technetium-99m labelled somatostatin analogs are also available. As an imaging method, PET has been repeatedly shown to surpass SPECT. The limitations of SPECT are lower spatial resolution, low sensitivity in detecting small tumors and high background activity in normal organs in comparison with PET. Also, PET has shorter investigation time and lower radiation burden. Hence, PET-CT should be used over SPECT whenever available. (Shah

et al., 2021; Hope *et al.*, 2023) The indications and their corresponding PET radiotracers are collected in Table 3.

2.2.3.1 GASTROENTEROPANCREATIC NEUROENDOCRINE NEOPLASMS

Neuroendocrine neoplasms account for approximately 1-1.5% of all gastroenteropancreatic neoplasms. GEP-NEN are defined into three groups according to the WHO grading system which was previously introduced. The system is based on Ki67 proliferation index and differentiation. (Kauhanen *et al*., 2020; Rindi *et al.*, 2022). GEP-NEN are most commonly located in the appendix (35% of all NEN), small intestine, and rectum but also pancreas, colon, and stomach. (Arola, Haglund and Välimäki, 2010) PET imaging has an important role in the diagnostics and therapeutics of GEP-NEN. Different imaging modalities are optimal for well and poorly differentiated GEP-NEN. (Kauhanen *et al*., 2020)

The most established imaging modality is ^{68}Ga-labeled somatostatin analog (SSA) PET-CT which is made possible by the wide expression of SSTR (80-100% of GEP-NET). Predominantly GEP-NET express the SSTR subtype 2. The tracers ^{68}Ga-DOTATATE, ^{68}Ga-DOTATOC and ^{68}Ga-DOTANOC are regarded as equally efficient. On the other hand, SSTR PET/CT has relatively low detection rate for poorly differentiated GEP-NET. The modified glucose molecule ^{18}F-FDG is suitable for imaging of poorly differentiated GEP-NEN. (Kauhanen *et al*., 2020; Rindi *et al.*, 2022). SSTR-PET has an important role in tumor staging, diagnosis of recurrencies, and therapeutics of GEP-NEN. (Janson *et al.*, 2021) When planning a surgical resection of the tumor SSTR-PET should have been done to all patients as the anatomical findings are important when planning the surgery. (Kauhanen *et al*., 2020)

Considering the small intestine, the amount of NEN has tripled during the past three decades. Currently, NEN is the most common neoplasm of the small intestine. A typical setting is a sporadic NEN in the end of the small intestine, the ileum. (Kauhanen *et al*., 2020) Typically, the tumors stain positive for serotonin and the Ki-67 index is 1-5%. (Janson *et al.*, 2021) At the time of the diagnosis, over 60% of cases have metastasized. (Kauhanen *et al*., 2020) Common locations for metastases are the liver as well as mesenteric and para-aortal lymph nodes. (Janson *et al.*, 2021) Small, multiple and metastasized

disease poses challenges for imaging. (Kauhanen *et al*., 2020) CT or MRI and SRI should always be performed.

Pancreatic neuroendocrine tumors (PNET) consist of 1-2% of all pancreatic tumors. PNET can be sporadic or linked to hereditary syndromes such as MEN1 and von Hippel – Lindau. (Kauhanen *et al*., 2020) Around 20-30% of PNET secrete hormones. Functional PNET secrete most commonly insulin or gastrin, but can also secrete glucagon, VIP, and somatostatin for example. Apart from insulinomas, PNET have significant malignant potential. The rest 70-80% of PNET are non-functional. The functionality of a tumor counts when choosing a suitable radiotracer for imaging. If thin needle biopsy is available, the selection is based on proliferation index. SSTR-PET is the first-hand imaging modality, but for high index values, ^{18}F-FDG is recommended. (Kauhanen *et al*., 2020; Janson *et al.*, 2021)

For some GEP-NEN endoscopy is sufficient diagnostic and therapeutic tool. Esophageal NEN are extremely rare (<1% of all NEN) with the majority being poorly differentiated NEC. When esophageal NEN is found it is most commonly an incidental finding during endoscopy. (Janson *et al.*, 2021). Same applies to gastric NEN which are typically found in gastroscopy. Gastric NEN are uncommon tumors with variable differentiation and malignant potential. Clinically, they are often linked to hypergastrinemia. Gastric NEN can be divided into three subtypes: type I, associated with autoimmune gastritis, type II, related to MEN1 and Zollinger-Ellison syndromes and type III, sporadic. For small and indolent gastric NEN type I, endoscopy is sufficient. For types II and III as well as large and high-grade NEN, also imaging is recommended. (10)

2.2.3.2 LUNG-NEN

Lung-NEN are common accounting for roughly 20% of all primary tumors of the lungs. Lung-NEN are classified differently from the general classification of NEN. These lung tumors are also divided into well-differentiated NET and poorly differentiated NEC, but they are further classified as typical carcinoid (TC) and atypical carcinoid (AC). On the other hand, lung-NEC is separated into small cell lung carcinoma (SCLC) and large cell neuroendocrine carcinoma (LCNEC). Though, LCNEC and carcinoids are significantly

more rare accounting for 3% and 2% respectively whereas SCLC accounts for 13-15% of all lung-NEN. (Dam *et al.*, 2023)

In the diagnostics of lung-NEN, PET-CT with ^{68}Ga-DOTATE or ^{68}Ga-DOTATOC is recommended. They have been shown to have comparable diagnostic accuracy. ^{64}Cu-DOTATATE might have some advantages over ^{68}Ga-DOTATE in the detection of lesions though sensitivity is the same. Additionally, ^{18}F-FDG PET-CT has a role in the identification of discordant lesions as FDG positive lesions tend to be SRI negative and the other way around. Considering peptide receptor radionuclide therapy (PRRT), that takes advantage of SSTR, a dual imaging with SRI and ^{18}F-FDG should be performed. This may add value in finding possible mismatching lesions which are a contraindication to PRRT. (Dam *et al.*, 2023)

2.2.3.3 INSULINOMA

The most common cause of hyperinsulinemic hypoglycaemia (HH) is an insulin producing insulinoma of the pancreas. HH is defined by low plasma glucose level as insulin is uncontrollably produced: the diagnostic criteria are serum insulin ≥3 μIU/ml and c-peptide ≥0.6 ng/mL while on a mixed meal test or on a 72-hour fast test with symptomatic patients. The incidence of insulinoma is approximately 4 cases per 1 million people. The other cause for HH is nesidioblastosis which is a hyperplasia of pancreatic beta-cells. For both causes of HH, the treatment is surgical making the localization of the lesion highly important. Here molecular imaging comes into play. (Kauhanen *et al*., 2020; Shah *et al.*, 2021)

Glucagon-like peptide-1 receptor (GLP-1R) based imaging has presented with higher sensitivity for the detection of insulinomas compared with other imaging modalities. Insulinomas have lower expression of SSTR compared with other NEN (60-70% of insulinomas) but express widely glucagon-like-peptide-1 receptor (GLP-1R). Exendin-4 is an agonist to GLP-1R. ^{68}Ga-exendin-4 PET-CT has presented with be the most sensitive (94%) and specific (83%) in the imaging of insulinomas compared with other anatomical and functional imaging modalities. With malign insulinomas (around 1/10 of insulinomas), the sensitivity of GLP-1R imaging is poorer (33.3%) due to lower expression of the receptors. (Shah *et al.*, 2021)

The current limitations of exendin-4 imaging are false positive uptakes of Brunner's gland, normal pancreas, and other beta-cell pathologies such as nesidioblastosis and false negatives in lesions of the pancreatic tail and malign insulinomas. Nesidioblastosis can also present with true negative uptakes due to the variation of GLP-1R expression. As the treatment strategies between nesidioblastosis (pancreatectomy) and insulinoma (enucleation) vary considerably, differentiation of the two is of great importance. (Shah *et al.*, 2021)

2.2.3.4 PARAGANGLIOMA AND PHAEOCHROMOCYTOMA

Phaeochromocytomas are NEN that rise in the adrenal gland and secrete adrenalin and noradrenalin. The same type of tumor rising outside the adrenal gland is referred to as paraganglioma. Paragangliomas can also present with signs of infiltration or compression of adjacent structures (tinnitus, dysphagia, hearing loss, and cranial nerve palsies). Phaeochromocytomas and paragangliomas (PPGL) are often benign and curable by surgical treatment. Approximately 10-20% of PPGL are metastatic. Some of PPGL are hereditary. They have been linked to over 20 different genetic mutations of which succinate dehydrogenase subunit (SDHx) mutations are most common. The tumor's uptake of different radiotracers is influenced by its genetic status. Plasma or urinary metanephrine levels are used in the diagnostics of PPGL. Metanephrine is the metabolite of adrenalin also known as epinephrine. (Taïeb *et al.*, 2019; Kauhanen *et al*., 2020)

The first-line imaging modality of PPGL is anatomical imaging. PPGL show avid enhancement on CT and MRI. Yet, nuclear imaging is more specific for theses tumors than anatomical imaging. Many PET tracers can be used in the imaging of PPGL such as ^{68}Ga-DOTA-SSA, ^{18}F-DOPA and ^{18}F-FDG. Almost all PPGL express SSTR which is why they are best found with ^{68}Ga-labelled SSA PET. ^{68}Ga-DOTA-SSA has been shown to have a pooled detection rate of 93%. ^{18}F-DOPA detected 80% and ^{18}F-FDG 74% of PPGL. Also, SPECT with indium-111-labelled pentetreotide or iodine-123-metaiodobenzylguanidine (MIBG) is widely used in the imaging of paraganglioma and phaeochromocytomas. Though, $^{123/131}$I-MIBG finds only 38% of cases. Besides diagnostics, and staging nuclear

imaging can also be used for the evaluation of suitability for PRRT as well as for the assessment of response to therapy. (Taïeb *et al.*, 2019)

Although ^{18}F-DOPA was formerly widely established, it's use today is limited to the imaging of phaeochromocytoma. ^{18}F-DOPA has the advantage of limited uptake of normal adrenal glands compared with other radiopharmaceuticals. Thus, ^{18}F-DOPA may be more efficient in the detection of phaeochromocytomas compared with ^{68}Ga-DOTA-SSA. Also, the tumor's uptake of different tracers is influenced by its genetic status. ^{18}F-DOPA might perform better in von Hippel – Lindau, HIF2A, FH, PHD1/2, and MAX mutations. ^{18}F-FDG could also be of use with certain mutations, such as SDHx and HIF2A. Overall, radiotracers ^{18}F-DOPA and ^{68}Ga-DOTA-SSA perform best in the imaging of phaeochromocytomas and paragangliomas. (Taïeb *et al.*, 2019; Kauhanen *et al*., 2020)

2.2.3.5 MEDULLARY THYROID CARCINOMA

Medullary thyroid carcinoma (MTC) covers 1-2% of all thyroid malignancies. MTC can be sporadic or hereditary being associated with the MEN2 syndrome. MTC originates from the parafollicular C cells of the thyroid gland. The parafollicular C cells secrete calcitonin and procalcitonin that can be used as serum tumor markers. The unspecific tumor marker CEA has value mainly in detecting disease relapse and progression after treatment. MTC diagnosis is reached with ultrasound of the neck and fine needle aspiration biopsy. The only curative treatment is total thyroidectomy. (Mäenpää *et al.*, 2010; Giovanella *et al.*, 2020)

PET-CT comes into the picture when detecting recurrent MTC. Also, PET-CT is useful in the detection of MTC metastases, the most common place being the lymph nodes of the neck, and in the assessment of the aggressiveness of the disease. PET-CT is not recommended for staging before treatment or for evaluating response to treatment. In follow-up of the disease, PET-CT of MTC is suggested when serum calcitonin exceeds 150 pg/ml or the calcitonin doubling time is shortened. Considering the PET imaging methods of MTC, three radiotracers rise above others: ^{18}F-DOPA, ^{18}F-FDG, and ^{68}Ga-labeled SSA. (Giovanella *et al.*, 2020)

^{18}F-DOPA has been shown to have the highest diagnostic performance of these three options. Therefore, it is recommended as the first line procedure for detecting recurrent MTC. The second-line procedure is imaging with ^{18}F-FDG. ^{18}F-FDG has been proven to be a powerful prognostic tool. Positivity with this modality predicts more aggressive disease and poorer prognosis. There are difficulties in the synthesis and acquisition of ^{18}F-DOPA and in such cases ^{18}F-FDG is recommended to be used instead. The diagnostic performance of ^{68}Ga-labeled SSA is significantly lower compared with other NEN due to MTC's variable expression of SSTR. ^{68}Ga-SSA PET-CT could be considered in selected cases with inconclusive imaging results or in the selection of patients suitable for SSTR-targeting therapies. Interestingly, studies suggest that early image acquisition, around 15 minutes after administration, in ^{18}F-DOPA imaging improves the detection rate of MTC in PET-CT. (Giovanella *et al.*, 2020)

Table 3. The indications of PET imaging of neuroendocrine neoplasms and the corresponding radiotracers. The most suitable tracer is presented first and is followed by the secondary choice.

Indication	**Radiotracer**
Well-differentiated gastroenteropancreatic NET	^{68}Ga-SSA
Poorly differentiated gastroenteropancreatic NEC	^{18}F-FDG
Lung NEN	^{68}Ga-SSA, ^{18}F-FDG
Phaeochromocytoma	^{18}F-DOPA, ^{68}Ga-SSA
Paraganglioma	^{68}Ga-SSA, ^{18}F-DOPA
Medullary thyroid carcinoma	^{18}F-DOPA, ^{18}F-FDG
Pancreatic insulinoma	^{68}Ga-SSA , Exendin-4

2.3 THERAPEUTICS

In therapeutic decision making several things are considered: symptoms and clinical findings, levels of biomarkers in blood and urine, genetic information, localization and staging of the primary tumor and histological confirmation which should always be obtained. Therapeutics options for the clinical management of advanced, metastasized, and progressive NEN are numerous: cytoreductive surgery, somatostatin analogs (SSA), chemotherapy, locoregional ablative therapies, peptide receptor radionuclide therapy (PRRT) and newer pharmaceuticals (such as everolimus and sunitinib). Here, the focus is on SSA and PRRT. (Basu *et al.*, 2020; Janson *et al.*, 2021)

2.3.1 SOMATOSTATIN ANALOGS

Somatostatin analogs (SSA) used in the treatment of NEN are octreotide (tradename Sandostatin) and lanreotide (tradename Somatuline). SSA target SSTR, which are overexpressed in most NEN, binding primarily to SSTR2 and SSTR5. SSA inhibit tumor growth and the release of gastrin, serotonin, vasoactive intestinal peptide, and other hormones and hormone metabolites. Traditionally, SSA are used in the treatment of secretory symptoms (such as flushing and diarrhea) of NEN. Long acting lanreotide LAR Depot has been shown to significantly prolong the time to progression (14.3 moths; 6 moths with placebo) of well-differentiated midgut NET that are unresectable. (Basu *et al.*, 2020)

Both SSA are available in short and long-acting formulations. Short-acting formulation of octreotide is administered as an immediate-release injection subcutaneously (sc.) (one ampoule contains 100 mcg) whereas the long-acting octreotide (LAR Depot) is injected intramuscularly (im) intragluteally once a month (recommended starting dose of 20mg). Lanreotide is available in a sustained-release formulation (Somatuline LA) that is injected every 10-14 days intramuscularly or in an extended-release formulation (Somatuline Autogel or Somatuline Depot) injected subcutaneously once a month. (Basu *et al.*, 2020)

2.3.2 PEPTIDE RECEPTOR RADIONUCLIDE THERAPY

Peptide receptor radionuclide therapy (PRRT) is an important treatment modality of advanced, metastasized, progressive, and well-differentiated inoperable NEN. It has been routinely included in the treatment of NEN only recently. According to the current guidelines, PET imaging should be performed to evaluate the eligibility to PRRT. PRRT is performed by administering intravenously an SSA labeled with a radiating isotope. PRRT targets somatostatin receptors, primarily SSTR2, thus SSTR positivity of the tumor is required. PRRT radionuclides deliver high dose of radiation directly to targeted neuroendocrine tumor cells expressing SSTR which damages these tumor cells. Generally, PRRT is well tolerated. Adverse effects include nausea, vomiting, and fatigue as well as hematologic and renal toxicity more rarely. Additionally, there exists a risk of acute precipitation of carcinoid syndrome known as carcinoid crisis. This phenomenon is more likely in

patients with large hepatic metastases and functioning, poorly controlled NEN. (Basu *et al.*, 2020; Fortunati *et al.*, 2023)

Current indications for PRRT are as follows: metastasized, advanced, or inoperable progressive, SSTR positive NET as well as functioning symptomatic NET that cannot be controlled by SSA, and high-grade NET when uptake is confirmed with SSTR imaging. The most common indication for PRRT is a metastatic GEP-NET. The response for PRRT is assessed in three scales which are improvement in health-related quality of life, biochemical response (reduction or increase in tumor markers), and imaging response. The most gratifying response, symptomatic improvement, has been seen in more than 80% of patients. Though, several factors have an impact on the response to the treatment which leads to varying individual results. (Basu *et al.*, 2020; Fortunati *et al.*, 2023).

Therapeutic radionuclides used for PRRT are ^{177}Lu-DOTATATE (lutetium-DOTA-(Tyr^3)-octreotate or lutetium oxodotreotide) and ^{90}Y-DOTATATE (or ^{90}Y-DOTATOC), the former being the most employed due to its favorable characteristics such as minimal adverse effects. Lutetium-177 and Yttrium-90 are beta emitters. For smaller tumors, ^{177}Lu-DOTATATE is preferred whereas ^{90}Y-DOTATATE is more suitable for larger tumors having higher beta particle energy. (Basu *et al.*, 2020). A phase 3 trial of the treatment of midgut NET with ^{177}Lu-DOTATATE showed promising results. In the study, patients were received either ^{177}Lu-DOTATATE and octreotide LAR or octreotide LAR alone. The progression free survival was markedly longer in the group receiving ^{177}Lu-DOTATATE. (Strosberg *et al.*, 2017, p. 3). Figure 1 illustrates these results.

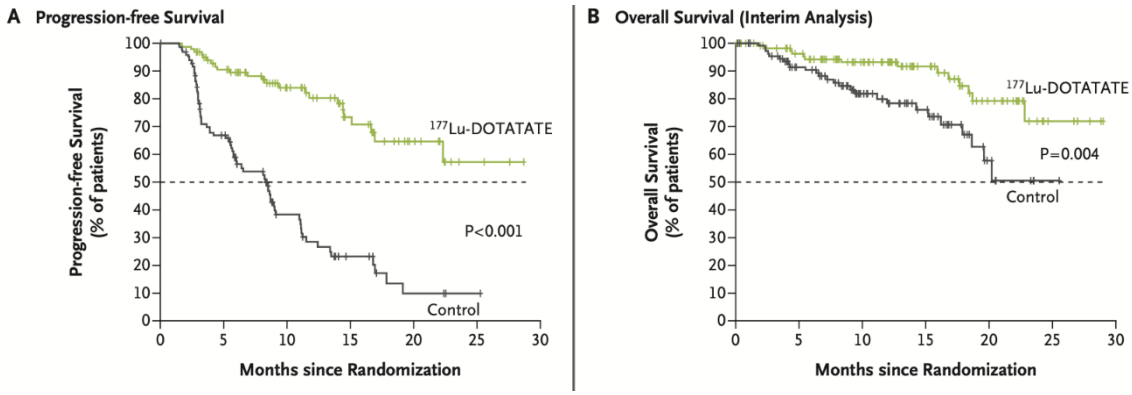

Figure 1. The progression-free (A) and overall survival (B) compared between ^{177}Lu-DOTATATE and control groups. (Strosberg *et al*., 2017)

There are several new radiotracers under investigation that could be used in PRRT of NEN in the future. ^{68}Ga-FAPI, a fibroblast activation protein inhibitor, is a novel radiopharmaceutical used in oncological imaging. Many case reports indicate high uptake of this radiotracer in NEN. More research is needed on its value to the clinical management of NEN with elevated levels of activated fibroblasts, though preliminary results are promising. Alpha-emitting ^{225}Ac-DOTATATE has been introduced for targeted alpha therapy of GEP-NET. Also, according to recent research, SSTR antagonists have some advantages over agonists such as the ability to identify more binding sites. (Fortunati *et al.*, 2023)

2.4 NEW RADIOTRACER ^{18}F-SiTATE

^{18}F-SiTATE is a novel PET radiotracer for imaging of well-differentiated NEN. It represents a promising alternative for the current golden standard, ^{68}Ga-labeled somatostatin receptor imaging (SRI). However, the use of ^{68}Ga-labeled radiotracer in PET-CT presents inherently economic and logistic challenges. The half-time of ^{68}Ga is relatively short (68 min), which hampers the commercial distribution of these tracers. Further, the tracer is obtained from costly and limitedly available on-site ^{68}Ge/^{68}Ga-generators. This enables the nuclear medicine physicians to practice scanning independently without cyclotrons or clean room facilities, but the low activity after single elution reduce the availability of ^{68}Ga-labeled radiotracers. Also, high mean β^+ energy impairs image resolution. Hence, alternatives for ^{68}Ga-labeled NEN imaging are highly welcome. (Ilhan *et al.*, 2020)

^{18}F-SiTATE has favorable characteristics which support its use over ^{68}Ga-DOTANOC. The longer half-life (110 min) and lower positron energy of the respective radiotracer enable advantageous patient logistics, efficient production, and high-resolution PET images. At present, the radiotracer has been evaluated in vitro and in animal studies as well as in humans. ^{18}F-labeled somatostatin analog shows comparable pharmacokinetic profile approaching the quality of ^{68}Ga-labeled radiotracers. ^{18}F-SiTATE is synthetically easily accessible, and the radiosynthesis is possible in a kit-like manner. To date, preliminary results show that ^{18}F-SiTATE PET-CT is a sensitive and specific molecular imaging

method in NEN patients for detection of somatostatin receptor positive lesions. (Ilhan *et al.*, 2020)

2.4.1 NON-CLINICAL STUDIES

Non-clinical ^{18}F-SiTATE studies have been conducted in vitro in human plasma and in tumor bearing mouse models. A mouse model was developed to be used in translating pre-clinical findings to clinical routine. The production of ^{18}F-SiTATE can be made fully in line with Good Manufacturing Practices (GMP). All animal experiments respected the National Guidelines for Animal Protection, Germany, and protocols of the local committee.

2.4.1.1 BIODISTRIBUTION IN MICE

The biodistribution of the new radiotracer [^{18}F]-SiFAlin-Asp$_3$-PEG$_1$-TATE ([^{18}F]SiFAlin currently known as ^{18}F-SiTATE) was investigated in AR42J tumor bearing mice by applying two physiologically based pharmacokinetic models. A SSTR2 based model, that was originally made for humans, was used to illustrate the data. Then, model 1 was modified by implementing receptor mediated endocytosis resulting in model 2. Parameters of the model were fitted to the biokinetic data of the mice. The model selection was performed by calculating Akaike weights using AICc (Akaike Information Criterion). The models illustrate the biodistribution of the radiotracer in the kidneys, liver, tumor, and whole body. (Maaß *et al.*, 2016)

The biodistribution of ^{18}F-SiTATE in mice was acquired from preclinical PET-CT data. An amount of 0.18±0.05 nmol (mean fluorine-18 activity of 4.8±1.3 MBq) of the radiotracer was injected as an infusion lasting 30 seconds for pre-therapeutic imaging. As discussed earlier, ^{18}F-SiTATE distributes through blood flow to the organs and binds to somatostatin receptors. Then, to determine the time-activity curves for tumor, kidneys, liver, and whole body, a software for the automated segmentation of organs of 4D PET-CT images was introduced. (Maaß *et al.*, 2016)

Figure 2 shows the typical biodistribution of ^{18}F-SiTATE. According to the data, model 2 is better supported by the data than model 1. Compared with humans, the density of

SSTR2 in the tumor is up to five-times higher and in the kidneys up to seven-times higher in the mouse model. Also, other parameter values were reported: blood flow (8.0±3.9 ml/min), hematocrit (0.47±0.04 a.u.), GFR (0.11±0.08) and the relative blood flow to the tumor (0.64±0.11 ml/min/g). (Maaß *et al.*, 2016)

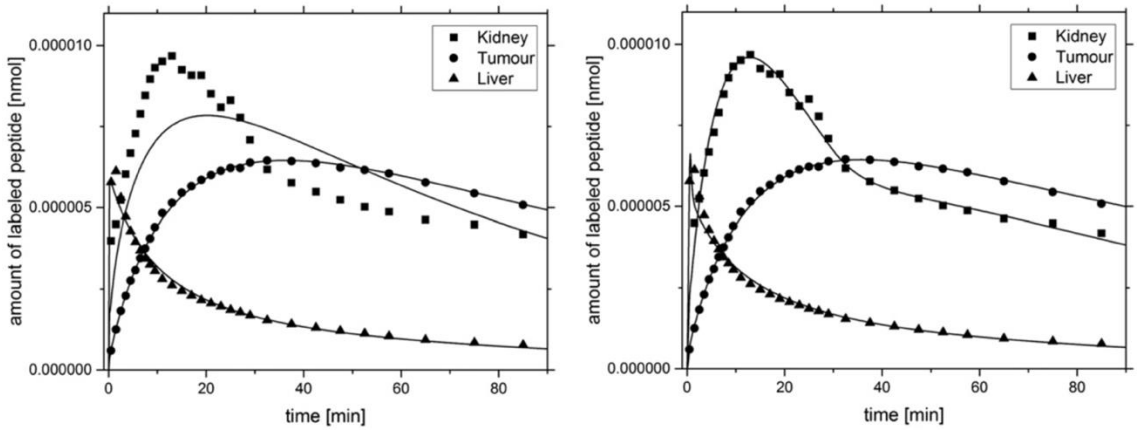

Figure 2. The human model (model 1, left) and the improved mouse model (model 2, right) presenting typical biodistribution of ^{18}F-SiTATE in the kidneys, liver, and tumor. The measurements are presented as dots and the model described as lines. (Maaß *et al.*, 2016)

2.4.1.2 IN VITRO EVALUATION

Firstly, the radiosynthesis of ^{18}F-SiTATE allows for production without special equipment or intricate procedures in a kit-like manner. The radiotracer was synthesized in high radiochemical yields of 52.5%±4.9% with activities of 44-63 GBq/µmol (starting activities: 3.3-6.7 GBq). Total synthesis time of only 20-25 minutes was achieved. The synthesis can be made fully in line with good manufacturing practice protocols. (Niedermoser *et al.*, 2015)

In vitro, the lipophilicity and stability of the radiotracer ^{18}F-SiTATE was tested in human serum. The serum stability determination was made mixing two hundred microliters of the radiotracer with 500 µl of human serum and then incubated at 37°C for 120 minutes. Competitive receptor binding affinity investigations were performed using viable AR42J rat carcinoma cells of the pancreas with known overexpression of SSTR. The radioactivity bound and internalized by the cells was determined using a gamma counter. By means of a non-linear regression algorithm, the inhibitory concentrations were calculated. (Niedermoser *et al.*, 2015)

In vitro human plasma studies showed no degradation of ^{18}F-SiTATE at 37°C over 120 min which indicates high stability. When compared with formerly developed SiFA-TATE derivates, a significant reduction in lipophilicity was discovered for the newer SiFA- and SiFAlin-derived somatostatin analogs. This decrease was explained with the aspartic acids introduced into the new TATE-derivates. The binding affinity of ^{18}F-SiTATE was investigated, and the results showed excellent inhibitory concentration values as well as a preserved binding affinity to somatostatin receptors. (Niedermoser *et al.*, 2015)

2.4.1.3 IN VIVO EVALUATION

In vivo properties of ^{18}F-SiTATE derivates were compared with the clinical reference standard. In the biodistribution experiments, an intravenous injection of the respective radiolabeled peptide (50µL; 1.1-5.3 MBq) was given to AR42J tumor bearing xenograft mice after which they were sacrificed at the time points of 60 or 90 minutes. The organs were dissected, and the activity of the tissues was measured using a gamma counter. In the mouse model, only renal excretion of ^{18}F-SiTATE was detected. (Niedermoser *et al.*, 2015)

Ex vivo biodistribution studies resulted in a comparable pharmacokinetic profile displaying a high and specific uptake in tumors and low physiological SSTR-positive organ accumulations. The maximum radioactivity accumulation in the tumor was 18.51±4.89 %ID/g 60 minutes after the injection. ^{68}Ga-DOTATATE was used as clinical reference standard. (Niedermoser *et al.*, 2015) For the biodistribution in the tumor bearing mice, see Figure 3.

When investigating ex vivo biodistribution at 90 minutes after the injection, the resulted tumor-to-blood ratio and tumor-to-muscle ratio were 57.58±35.89 and 211.05±143.38 respectively. The uptake in bone was 1.31±0.31 %ID/g at the same timepoint. From this finding, the high in vivo resistance of ^{18}F-SiTATE to ^{18}F-hydrolysis can be deduced. (Niedermoser *et al.*, 2015)

Animal PET studies were conducted with AR42J tumor bearing mice. The mice were injected with 4-8 MBq of ^{18}F-SiTATE to image the in vivo SSTR positive tumors. A

small animal PET/SPECT/CT scanner was used to acquire a dynamic scan and a CT image. The radiotracer SUV for the highest tumor accumulation 80-90 minutes after injection was 7.80. (Niedermoser *et al.*, 2015)

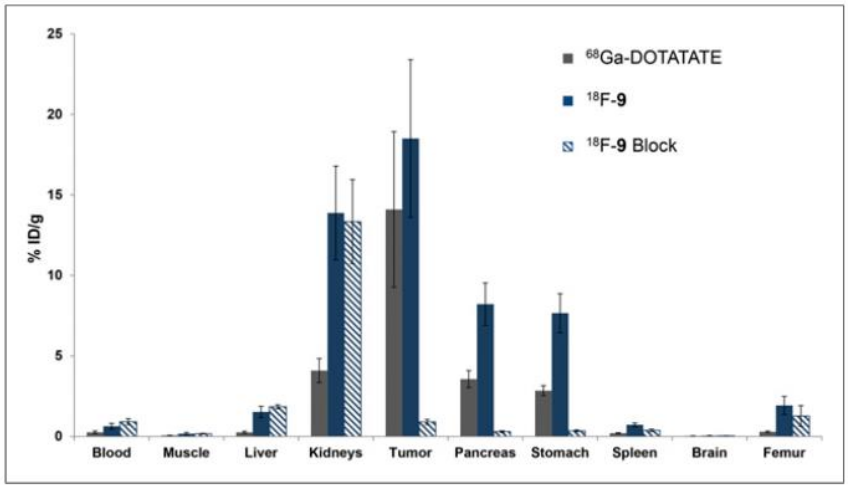

Figure 3. Biodistribution values of ^{18}F-SiTATE (^{18}F-9) in xenograft AR42J tumor bearing mouse model 60 minutes after injection (%ID/g). For ^{18}F-SiTATE, a blocking experiment was done using DOTATATE (220 µg/mouse; n=5). The figure shows specific binding to tumor and physiologically SSTR-positive organs. (Niedermoser *et al.*, 2015)

2.4.2 EFFECTS IN HUMANS

All procedures performed in the studies with human participants were done fully in compliance with the ethical standards of the institutional and/or national research committee (LMU Munich – approval number 20-1077) and with the Helsinki Declaration 1964 and its later amendments.

2.4.2.1 FIRST-IN-HUMAN TRIAL

The first-in-human trial of ^{18}F-SiTATE was conducted with a male patient with metastatic NEN of unknown primary. ^{18}F-SiTATE PET-CT scan showed highly comparable uptake values to a previously performed ^{68}Ga-DOTATOC scan. The SUV_{max} values of ^{18}F-SiTATE vs. ^{68}Ga-DOTATOC for three cardiac metastases were 15.6 vs. 9.5, 16.4 vs. 15.4, 12.6 vs. 17.6, and for a femur metastasis 55.9 vs. 24.3, respectively). Ga-labelled SRI is considered the current golden standard of NEN PET imaging. The results of the first in

human trial of the novel radiotracer were promising, and strongly support the use of ^{18}F-SiTATE for the PET-CT imaging of NEN patients. (Ilhan *et al.*, 2019)

2.4.2.2 BIODISTRIBUTION IN HUMANS

The first-in-human data provided valuable knowledge of the biodistribution of the novel radiopharmaceutical ^{18}F-SiTATE. The intra-individual biodistribution and tumor uptake were investigated with thirteen NEN-patients who underwent ^{18}F-SiTATE PET-CT (median 240±25 MBq). SUV_{max} and SUV_{mean} were calculated 1 hour after injecting the radiopharmaceutical. Analyses were performed retrospectively. The current clinical reference standard, ^{68}Ga-labeled radiotracer, was used as a reference point. Image quality was also assessed. (Ilhan *et al.*, 2020)

The highest SUV_{max} and SUV_{mean} values were achieved in the adrenal gland, the liver, the spleen, and the kidneys for ^{18}F-SiTATE. A statistically significantly higher SUV_{max} was noted in the kidneys, the myocardium, and the bone when compared with ^{68}Ga-DOTATOC. The tumor uptake values were calculated. Significantly higher SUV_{max} and SUV_{mean} in ^{18}F-SiTATE PET-CT were noted in almost all tumor lesions in comparison with ^{68}Ga-DOTATOC. (Ilhan *et al.*, 2020) For more detailed information see Figures 4 and 5.

Using quantitative data as an alternative for visual interpretation, the tumor-to-spleen ratio (TSR) and the tumor-to-liver ratio (TLR) of ^{18}F-SiTATE and ^{68}Ga-DOTATOC were compared in conformity with the Krenning score. All other $_{max}$TSR $_{max}$TLR values were comparable except the higher values of ^{18}F-SiTATE in myocardial metastases, lower $_{max}$TLR in lymph node metastases, and higher $_{max}$TSR in ovarian metastases. Image quality assessments and an intra-class correlation (ICC) analysis resulted in almost-perfect agreement between the readers. (Ilhan *et al.*, 2020)

The results indicate ^{18}F-SiTATE being highly comparable with current golden standard of NEN PET-imaging. The comparable biodistribution to ^{68}Ga-DOTATOC and high tumor-to-normal-tissue ratio of ^{18}F-SiTATE are encouraging. The higher biodistribution of ^{18}F-SiTATE in normal organs compared with ^{68}Ga-DOTATOC is ascribed to the lipophilicity of the SiFA-group. (Ilhan *et al.*, 2020)

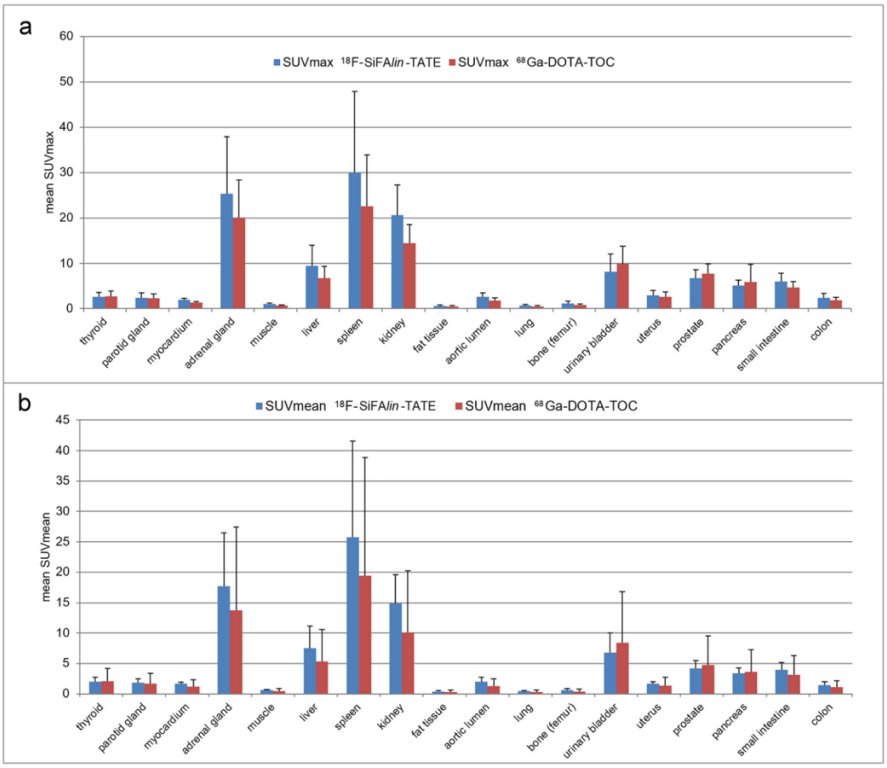

Figure 4. The biodistribution of ^{18}F-SiTATE and ^{68}Ga-DOTATOC in humans according to SUV_{max} (a) and SUV_{mean} (b) values 1h after the injection. (Ilhan *et al.*, 2020)

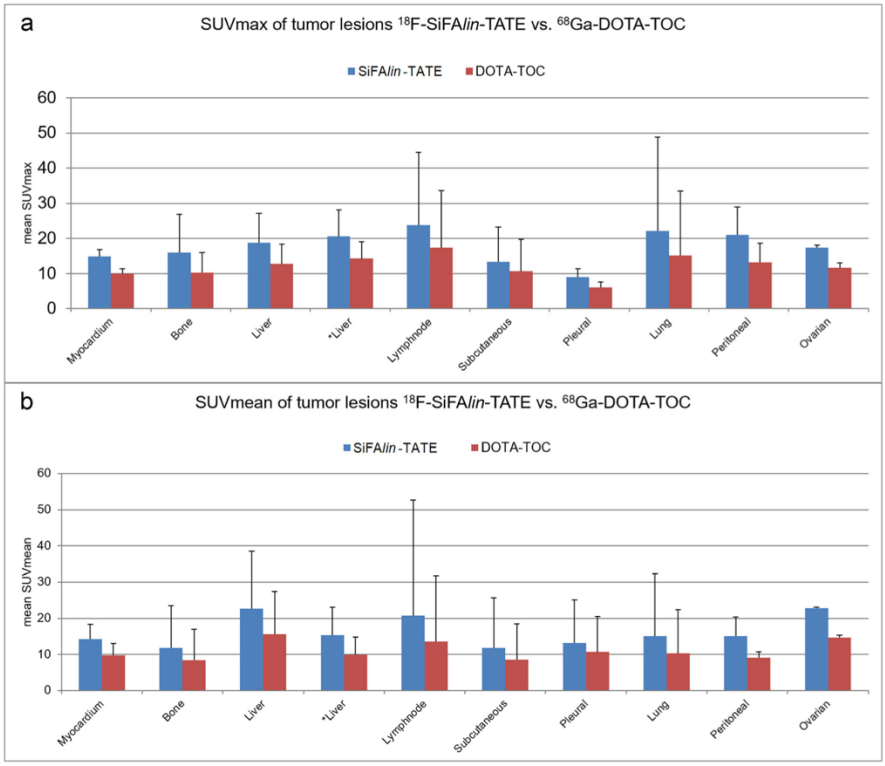

Figure 5. The tumor uptake values of ^{18}F-SiTATE and ^{68}Ga-DOTATOC: a) SUV_{max} and b) SUV_{mean}. In total, 109 lesions were analyzed. (Ilhan *et al.*, 2020)

2.4.2.3 HUMAN RADIATION DOSIMETRY AND OPTIMAL SCAN TIME

The human radiation dosimetry was investigated with repeated emission scans in eight NEN patients who received single intravenous injection of ^{18}F-SiTATE (250±66 MBq). The dosimetry estimates for organs at risk were defined using a linear-monoexponential model and applying ^{18}F S-values. All dosimetry values were reported in terms of the reference adult female and male organ masses (ICRP89). OLINDA 2.0 software was used for the calculations of the radiation doses. The software applies the Medical Internal Radiation Dose (MIRD) system. (Beyer *et al.*, 2021)

The accumulation of the radiotracer to normal organs did not significantly change between the time points of 1h and 3h post-injection. The highest SUV_{max} and SUV_{mean} for the normal organs were observed in the urinary bladder, the spleen, the kidneys, and the adrenal gland. For all SUV_{max} and SUV_{mean} of the normal organs, see Figure 6. The tumor-to-background ratios were shown to be excellent and, due to the progressively increasing uptake by tumors, leading to even higher ratios over time. SUV_{mean} tumor-to-liver ratios 60 min vs. 120 min were: 2.7±1.7 vs. 3.5±2.1, +28%; 60 vs. 180 min: 2.7±1.7 vs. 4.0±2.3, +48%; 120 vs. 180 min: 3.5±2.1 vs. 4.0±2.3, +16%). (Beyer *et al.*, 2021)

The primary locations of radioactive uptake in humans were the spleen, the kidneys, the adrenal glands, the liver, and the wall of the urinary bladder. The most affected organ was the spleen with an absorbed organ dose of 0.144 mSv/MBq. The total effective dose was 0.015±0.004 mSv/MBq. Therefore, the effective dose for a mean activity of 250 MBq was 3.8 mSv. The radiation exposure of ^{18}F-SiTATE was lower compared to the clinical reference standard, ^{68}Ga-labeled radiotracers. (Beyer *et al.*, 2021)

The image quality of ^{18}F-SiTATE was evaluated as good or excellent in 80% of the cases. The best compromise between tumor-to-background contrast and image quality was noted at 120 min and the second best at 60 min post-injection. The readers were in good agreement and no statistically significant differences were found. Figure 7 illustrates the high tumor-to-background contrast and image quality of ^{18}F-SiTATE (Beyer *et al.*, 2021)

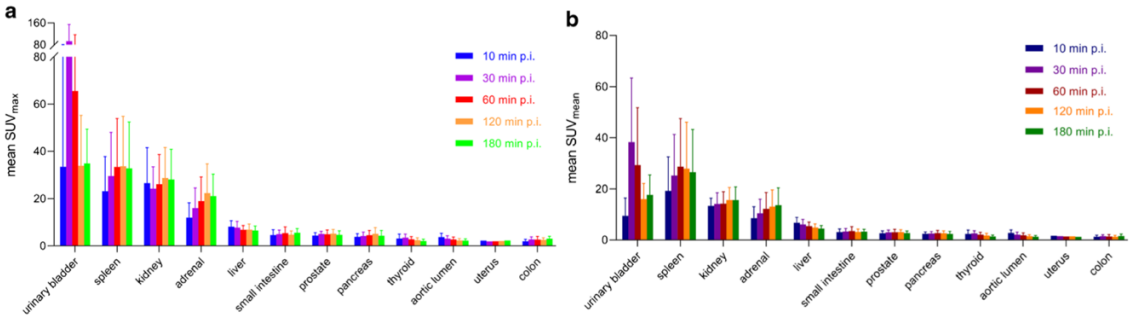

Figure 6. The biodistribution of ^{18}F-SiTATE over time: a) SUV_{max} and b) SUV_{mean} of normal organs in the time points of 10, 30-, 60-, 120-, and 180-min post-injection (p.i.). (Beyer *et al.*, 2021)

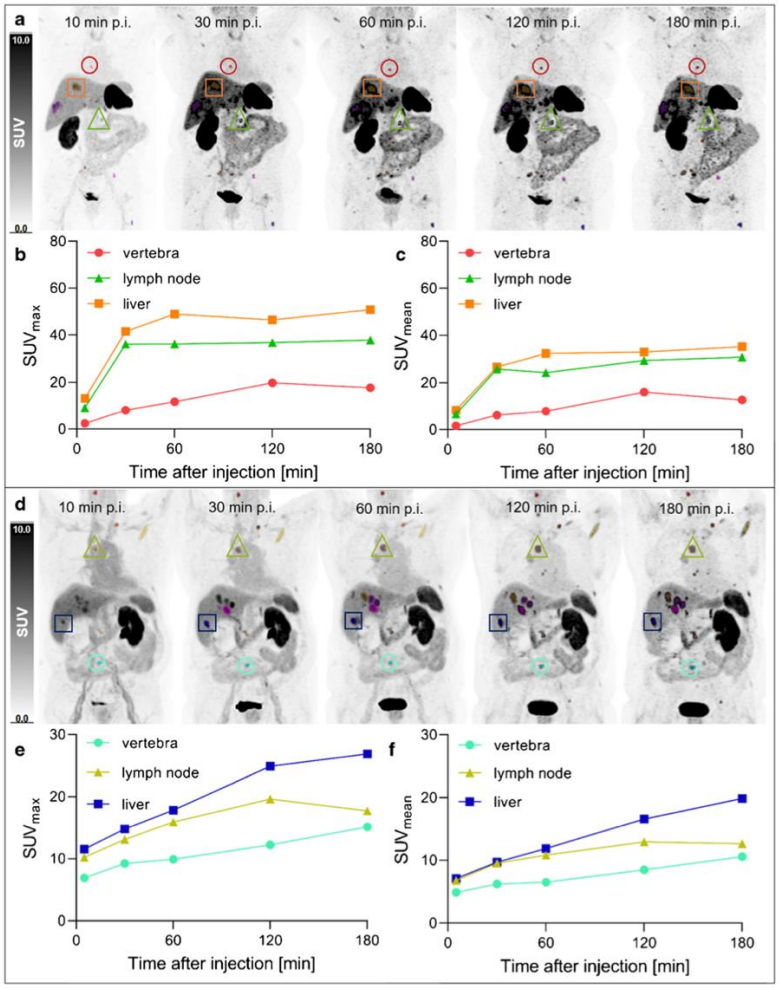

Figure 7. a, d) The maximum intensity projections in two exemplary patients at10, 30, 60, 120, 180 min post-injection with corresponding **b, e)** SUV_{max} and **c,f)** SUV_{mean} time-activity curves of three metastatic lesions; upper image: female, ^{18}F-SiTATE 114 MBq, no SSA medication; lower image: male, ^{18}F-SiTATE 316 MBq, SSA medication (Beyer *et al.*, 2021)

3 CONCLUSIONS

The goal of this literature review was to investigate the PET imaging methods of neuroendocrine neoplasms. Today, the golden standard is ^{68}Ga-labeled somatostatin analogue imaging. Several ^{68}Ga-labeled radiotracers have been developed, and these have been considered equally efficient in the detection of somatostatin receptor positive disease though they have varying affinity profiles to SSTR. According to the current guidelines, ^{68}Ga-labeled SSA imaging is recommended for diagnosis, restaging, and treatment monitoring of well-differentiated NEN. Another widely used radiotracer is ^{18}F-FDG, which has been shown to detect poorly differentiated and predict more aggressive forms of the disease. The use of ^{18}F-DOPA has declined but it still has a role at least in the imaging of medullary thyroid carcinoma and phaeochromocytoma.

New radiotracers are actively being developed for PET imaging of NEN. One of the latest developments is ^{68}Ga-exendin-4, which has presented with the highest detection rate for pancreatic insulinomas compared with other imaging modalities. The Turku PET Center took part in a multicenter trial that showed that exendin-4 is a viable tool in the diagnosis of hyperinsulinemic hyperglycemia. However, the widely used ^{68}Ga-labeled radiotracers present with some economic and logistic challenges creating the need for new radiopharmaceuticals with more suitable characteristics. A promising new alternative for the imaging of SSTR positive disease is ^{18}F-SiTATE, which is also being investigated in the Turku PET Center. First-line studies have presented with no side effects neither in mice models nor in humans. Recent studies indicate high tumor uptake values and high image quality, though clinical in-human data is still limited.

The cite of the primary tumor is relevant in determining the most appropriate radiopharmaceutical. NEN are most often met in the GI-tract. Well-differentiated gastroenteropancretic NEN are best detected with ^{68}Ga-labelled SSA whereas ^{18}F-FDG is suitable for poorly differentiated tumors. Lung NEN are imaged with^{68}Ga-labelled SSA to establish SSTR status but dual imaging with ^{18}F-FDG is recommended for the detection of discordant lesions. Phaeochromocytomas of the adrenal gland are detected with ^{18}F-DOPA or ^{68}Ga-labeled SSA but the first-mentioned might be more efficient than the latter. These radiotracers are also recommended for the imaging of paragangliomas. MIBG is today a widely used imaging method for phaeochromocytomas and paragangliomas while it has

a markedly lower detection rate. PET imaging of MTC is recommended for the detection of recurrencies and metastases. The imaging modalities are ^{18}F-DOPA, ^{18}F-FDG, and ^{68}Ga-labeled SSA of which the first mentioned has the highest diagnostic performance.

PET imaging of NEN is needed for the evaluation of appropriate therapies. PRRT is considered a safe and effective treatment option for NEN expressing SSTR. PET imaging should be performed prior to PRRT to evaluate the eligibility for the treatment. ^{177}Lu-DOTATATE is the preferred radiopharmaceutical due to its favorable characteristics, but ^{90}Y-DOTATATE is also in use. Currently, several radiotracers are under investigation to study whether they could be used in PRRT in the future. Many case reports indicate that the novel ^{68}Ga-FAPI has high uptake in NEN, but more research is needed on its clinical value. Besides PET imaging, SSA are traditionally used in treatment of secretory symptoms of NEN as an intramuscular or subcutaneous injection.

The medical field shows great interest in PET imaging today. PET imaging of NEN is under eager investigations. There are several novel radiotracers under development for the diagnostics of NEN besides the plethora of already established radiotracers in active use. ^{68}Ga-labelled radiotracers present with economic and logistic challenges, so new solutions are needed. More studies are needed of the efficacy of ^{18}F-SiTATE and its capability to possibly replace the current golden standard. Also, the value of radiopharmaceuticals in the treatment of NEN patients should not be forgotten. The Turku PET Center is a central place for PET imaging studies in Finland but also on an international level.

4 REFERENCES

Aittomäki, K. and Peltomäki, P. (2016) 'Periytyvä syöpäalttius', in *Lääketieteellinen genetiikka*. Duodecim.

Arola, J., Haglund, C. and Välimäki, M. (2010) 'Ruuansulatuskanavan ja haiman endokriiniset kasvaimet', in *Endokrinologia*. Duodecim.

Basu, S. *et al.* (2020) 'Peptide Receptor Radionuclide Therapy of Neuroendocrine Tumors', *Seminars in Nuclear Medicine*, 50(5), pp. 447–464.

Beyer, L. *et al.* (2021) 'Dosimetry and optimal scan time of [18F]SiTATE-PET/CT in patients with neuroendocrine tumours', *European Journal of Nuclear Medicine and Molecular Imaging*, 48(11), pp. 3571–3581.

Bozkurt, M.F. *et al.* (2017) 'Guideline for PET/CT imaging of neuroendocrine neoplasms with 68Ga-DOTA-conjugated somatostatin receptor targeting peptides and 18F-DOPA', *European Journal of Nuclear Medicine and Molecular Imaging*, 44(9), pp. 1588–1601.

Dam, G. *et al.* (2023) 'Nordic 2023 guidelines for the diagnosis and treatment of lung neuroendocrine neoplasms', *Acta Oncologica*, 62(5), pp. 431–437.

Fortunati, E. *et al.* (2023) 'Molecular imaging Theranostics of Neuroendocrine Tumors', *Seminars in Nuclear Medicine*, 53(4), pp. 539–554.

Giovanella, L. *et al.* (2020) 'EANM practice guideline for PET/CT imaging in medullary thyroid carcinoma', *European Journal of Nuclear Medicine and Molecular Imaging*, 47(1), pp. 61–77.

Hofland, J. *et al.* (2019) 'Management of carcinoid syndrome: a systematic review and meta-analysis', *Endocrine-Related Cancer*, 26(3), pp. R145–R156.

Hogg, P. and Testanera, G. (eds) (2010) *Principles and Practice of PET/CT*. European Association of Nuclear Medicine.

Hope, T.A. *et al.* (2023) 'SNMMI Procedure Standard/EANM Practice Guideline for SSTR PET: Imaging Neuroendocrine Tumors', *Journal of Nuclear Medicine*, 64(2), pp. 204–210.

Ilhan, H. *et al.* (2019) 'First-in-human 18F-SiFAlin-TATE PET/CT for NET imaging and theranostics', *European Journal of Nuclear Medicine and Molecular Imaging*, 46(11), pp. 2400–2401.

Ilhan, H. *et al.* (2020) 'Biodistribution and first clinical results of 18F-SiFAlin-TATE PET: a novel 18F-labeled somatostatin analog for imaging of neuroendocrine tumors', *European Journal of Nuclear Medicine and Molecular Imaging*, 47(4), pp. 870–880.

Inzani, F. and Rindi, G. (2021) 'Introduction to neuroendocrine neoplasms of the digestive system: definition and classification', *Pathologica*, 113(1), pp. 1–4.

Janson, E.T. *et al.* (2021) 'Nordic guidelines 2021 for diagnosis and treatment of gastroenteropancreatic neuroendocrine neoplasms', *Acta Oncologica*, 60(7), pp. 931–941.

Kauhanen, S. *et al*. (2020) 'Endokriinisten sairauksien PET-kuvantaminen', Duodecim (136), pp. 1086–94.

Komar, G. (2012) *Imaging of tumour microenvironment for the planning of oncological therapies using positron emission tomography*. University of Turku.

Maaß, C. *et al.* (2016) 'Physiologically based pharmacokinetic modeling of 18F-SiFAlin-Asp3-PEG1-TATE in AR42J tumor bearing mice', *Nuclear Medicine and Biology*, 43(4), pp. 243–246.

Mäenpää, H. *et al.* (2010) 'Kilpirauhasen kasvaimet', in *Endokrinologia*. Duodecim.

Niedermoser, S. *et al.* (2015) 'In Vivo Evaluation of ^{18}F-SiFA *lin* –Modified TATE: A Potential Challenge for ^{68}Ga-DOTATATE, the Clinical Gold Standard for Somatostatin Receptor Imaging with PET', *Journal of Nuclear Medicine*, 56(7), pp. 1100–1105.

Pietrzak, A. (ed.) (2021) *Advances in PET-CT imaging: a technologist's guide*. European Association of Nuclear Medicine.

Rindi, G. *et al.* (2022) 'Overview of the 2022 WHO Classification of Neuroendocrine Neoplasms', *Endocrine Pathology*, 33(1), pp. 115–154.

Shah, R. *et al.* (2021) 'Exendin-4-based imaging in insulinoma localization: Systematic review and meta-analysis', *Clinical Endocrinology*, 95(2), pp. 354–364.

Silvoniemi, A. (2018) *Novel aspects for methodology and utilization of PET/CT imaging in head and neck cancer*. University of Turku.

Strosberg, J. *et al.* (2017) 'Phase 3 Trial of ^{177}Lu-Dotatate for Midgut Neuroendocrine Tumors', *New England Journal of Medicine*, 376(2), pp. 125–135.

STUK. n.d. Environmental radiation (2024). Accessed: 26 January 2024. https://stuk.fi/en/environmental-radiation.

Taïeb, D. *et al.* (2019) 'European Association of Nuclear Medicine Practice Guideline/Society of Nuclear Medicine and Molecular Imaging Procedure Standard 2019 for radionuclide imaging of phaeochromocytoma and paraganglioma', *European Journal of Nuclear Medicine and Molecular Imaging*, 46(10), pp. 2112–2137.